

Chaos and the continuum limit in the gravitational N -body problem. I. Integrable potentials

Henry E. Kandrup*

Department of Astronomy, Department of Physics, and Institute for Fundamental Theory
University of Florida, Gainesville, Florida 32611

Ioannis V. Sideris†

Department of Astronomy, University of Florida, Gainesville, Florida 32611
(October 29, 2018)

This paper summarises a numerical investigation of the statistical properties of orbits evolved in ‘frozen,’ time-independent N -body realisations of smooth, time-independent density distributions corresponding to integrable potentials, allowing for $10^{2.5} \leq N \leq 10^{5.5}$. Two principal conclusions were reached: (1) In the limit of a nearly ‘unsoftened’ two-body kernel, *i.e.*, $V(r) \propto (r^2 + \epsilon^2)^{-1/2}$ for small ϵ , the value of the largest Lyapunov exponent χ does *not* appear to decrease systematically with increasing N , so that, viewed in terms of the sensitivity of individual orbits to small changes in initial conditions, there is no sense in which chaos ‘turns off’ for large N . (2) Nevertheless, there is a clear, quantifiable sense in which, on the average, as N increases chaotic orbits in the frozen- N systems come to more closely resemble integrable characteristics in the smooth potential. When viewed in configuration or velocity space, or as probed by collisionless invariants like angular momentum, frozen- N orbits typically diverge from smooth potential characteristics as a power law in time on a time scale $\propto N^p t_D$, with t_D a characteristic dynamical, or crossing, time. For the case of angular momentum, the divergence is well approximated by a $t^{1/2}$ dependence, so that, when viewed in terms of collisionless invariants, discreteness effects acts as a diffusion process which, presumably, can be modeled by nearly white Gaussian noise in the context of a Langevin or Fokker-Planck description. For position and velocity, the divergence is somewhat more rapid and characterised by a t^q power law growth with $q \approx 1$, a result that likely reflects the effects of linear phase mixing.

PACS number(s): 05.60.+w, 51.10.+y, 05.40.+j

I. INTRODUCTION AND MOTIVATION

Many astronomical objects, including, *e.g.*, globular clusters, are typically modeled by bulk gravitational potentials which manifest a high degree of symmetry and which, being integrable, lead to completely regular characteristics with no possibility of chaotic behaviour. One knows, however, that such bulk potentials constitute idealisations, the true system corresponding (at least approximately) to a realisation of the gravitational N -body problem. The important point, then, is that motion in the N -body problem, even for an N -body system which samples a smooth, time-independent phase space distribution corresponding to an integrable potential, is typically chaotic in the sense that orbits exhibit exponential sensitivity towards small changes in initial conditions [1]. This perhaps is not surprising. The true potential associated with a collection of point masses no longer possesses the symmetries of the original integrable potential, so that there is no reason why the orbits should not be chaotic.

However, what *is*, perhaps, surprising is the expectation, derived both from theoretical arguments [2,3] and from numerical simulations [4], that the N -body problem remains chaotic even for very large N . Suppose, *e.g.*, that a system of total mass $M = 1$ is represented by a collection of N objects of mass $m = 1/N$, so distributed as to sample the density distribution corresponding to an

integrable potential. The claim then is that, when expressed in units of a natural dynamical, or crossing, time $t_D \sim 1/\sqrt{G\rho}$, with ρ a typical density, the characteristic time scale τ on which an initial perturbation in any given orbit tends to grow will not diverge for $N \rightarrow \infty$. In this sense, the degree of chaos manifested by individual orbits is not expected to ‘turn off’ for very large N . There is an apparent consensus, motivated both from theory and numerical experiments, that τ should not increase without bound for $N \rightarrow \infty$, although there is some disagreement in the literature as to whether $\tau(N)$ should converge towards an N -independent value [2] or whether τ should instead slowly *decrease* with increasing N [3].

If, however, this be true, one is confronted with subtle questions of principle regarding the nature of the continuum limit. It is generally assumed [5] that, for sufficiently large N , a self-gravitating system of discrete point masses can be characterised adequately by a smooth phase space density that solves the collisionless Boltzmann equation (*CBE*), *i.e.*, the gravitational analogue of the Vlasov equation from plasma physics. The obvious point, then, is that time-independent solutions to this equation which manifest a high degree of symmetry correspond typically to bulk potentials which are integrable or, even if they be nonintegrable, admit large measures of regular orbits. But how is one to reconcile integrable or near-integrable behaviour in such bulk potentials with the presumed fact that, even for very large N , individual orbits in the true

N -body problem typically manifest chaotic behaviour on a time scale $\sim t_D$?

Strictly speaking, there is no logical contradiction: It is completely possible for collective properties of an N -body system to be described correctly by the *CBE*, even if the characteristics associated with the self-consistent potential do not coincide, even approximately, with real N -body trajectories. However, it *would* seem important to pin down carefully what is actually going on:

- Is it really true that individual trajectories in the N -body problem are chaotic for very large N , even if the bulk potential associated with the system is integrable? The indications are that the answer to this is: yes. However, most of the work done to date on chaos in the N -body problem has focused on systems with comparatively small N and/or a hierarchy of masses, or, for larger systems, on comparatively short time behaviour. Little if any work has been done to provide estimates of honest Lyapunov exponents over intervals $\gg t_D$ for large N systems comprised of bodies of comparable mass.
- Does this chaos reflect simply the fact that the system is grainy, or does it reflect the details of the full N -body dynamics? If, *e.g.*, one were to replace a smooth time-independent, integrable potential by the irregular potential associated with an N -particle sampling of the smooth mass density that is frozen in time, to what extent will motion in that grainy time-independent potential be chaotic?
- Even presuming that the N -body problem is chaotic on a time scale $\sim t_D$, is there some well defined sense in which the ‘average’ properties of individual N -body trajectories track characteristics given by the *CBE*?

These conceptual issues are also related directly to the problem of ‘softening.’ It is generally recognised that, for small N , close encounters between individual masses are more important dynamically than for larger N [5]. For this reason, N -body simulators interested in exploring the physics of the N -body problem for larger N often suppress the effects of close encounters artificially by replacing the true $1/r$ potential by a softened potential $V(r) \propto (r^2 + \epsilon^2)^{-1/2}$ for some ‘softening parameter’ ϵ . This certainly suppresses encounters with impact parameters $< \epsilon$ which, presumably, is a good thing. However, there are strong indications [6] that orbits integrated with such a softened potential tend to be ‘less chaotic’ in their behaviour, so that the introduction of softening also has the potentially undesirable effect of removing N -body chaos which really ought to be present, even for very large N . In any event, earlier investigations of chaos in the N -body problem based on simulations which incorporate a large amount of softening must be viewed with suspicion, since such simulations could suppress precisely the effects which one might wish to explore!

This paper summarises a detailed exploration of chaos in time-independent potentials generated by sampling the smooth density $\rho(\mathbf{r})$ associated with a time-independent solution to the *CBE* to create a frozen N -body realisation of that equilibrium. Most of the work

focuses on the particularly simple case of an integrable Plummer potential [5], which derives from a spherically symmetric mass distribution. However, it was also confirmed that, modulo one point discussed in the concluding section, the same qualitative results obtain for the potential associated with a constant density spherical configuration.

Section II begins by describing the numerical experiments that were performed. Section III summarises a computation of *honest* Lyapunov exponents in frozen N -body realisations of the Plummer potential, exploring how the largest exponent χ associated with representative initial conditions varies as a function of ϵ and N . The principal conclusion here is that, at least for small values of ϵ , orbits in such potentials are invariably chaotic; and that, even for particle number as large as $N = 10^5$, there is no sense in which increasing N ‘turns the chaos off.’ Section IV demonstrates that, even though the Lyapunov exponents do not decrease with increasing N , there is a well defined sense in which, as N increases, orbits in frozen- N potentials remain ‘close’ to smooth potential characteristics with the same initial condition for progressively longer times. Section V concludes by summarising the principal conclusions, providing a simple physical interpretation, and then commenting on potential implications.

The principal conclusion of this paper is that, for integrable smooth potentials which admit no chaos, the continuum limit makes sense even at the level of pointwise properties of individual trajectories. The possibility of chaotic characteristics leads necessarily to very different behaviour and, for this reason, the case of nonintegrable potentials that admit both regular and chaotic characteristics will be considered in a separate paper.

II. DESCRIPTION OF THE NUMERICAL EXPERIMENTS

The numerical computations reported here were performed for a so-called Plummer potential,

$$\Phi(r) = -\frac{GM}{\sqrt{r^2 + b^2}}. \quad (2.1)$$

This potential is generated via Poisson’s equation from a density profile

$$\rho(r) = \left(\frac{3M}{4\pi b^3} \right) \left(1 + \frac{r^2}{b^2} \right)^{-5/2}, \quad (2.2)$$

and corresponds to an equilibrium solution to the *CBE* satisfying

$$f(E) = \begin{cases} A(-E)^{7/2} & \text{if } \Phi(r=0) < E = \frac{1}{2}v^2 + \Phi < 0; \\ 0 & \text{if } E = \frac{1}{2}v^2 + \Phi > 0. \end{cases} \quad (2.3)$$

Units were so chosen that $G = M = b = 1$.

The principal aim was to compare orbits generated in the smooth potential with orbits evolved in time-independent N -body realisations of the potential. For a variety of fixed values of N and ϵ , 20 different time-independent N -body potentials were constructed. Each of these was associated with a random sampling of the smooth density distribution generated using a von Neumann rejection algorithm (cf. [7]). This entailed constructing singular density distributions

$$\rho_N(\mathbf{r}) = \frac{M}{N} \sum_{i=1}^N \delta_D(\mathbf{r} - \mathbf{r}_i), \quad (2.4)$$

which, allowing for a softening parameter ϵ , yielded potentials of the form

$$V_N(\mathbf{r}) = -\frac{GM}{N} \sum_{i=1}^N \frac{1}{\sqrt{(\mathbf{r} - \mathbf{r}_i)^2 + \epsilon^2}}. \quad (2.5)$$

The objective then was to select individual initial conditions $(\mathbf{r}_0, \mathbf{v}_0)$ and to evolve these initial conditions in both the smooth potential and the 20 ‘frozen’ N -body potentials, while simultaneously tracking the evolution of a small initial perturbation, periodically renormalised at fixed intervals δt , so as to extract an estimate of the largest (short time) Lyapunov exponent [8].

The integrations were performed for a time corresponding physically to $\sim 100t_D$ using a Runge-Kutta integrator that typically conserved energy to at least one part in 10^4 . The value $100t_D$ was selected (i) because it corresponded to an interval sufficiently long that one began to see convergence towards a well-defined Lyapunov exponent χ and, perhaps more importantly, (ii) because, for physical systems like real galaxies, $100t_D$ corresponds to an interval comparable to the age of the Universe.

The total particle number N in the ‘frozen’ N -body potentials was allowed to vary between $N = 10^{2.5}$ and $N = 10^{5.5}$. Physical interest focuses primarily on the limit $\epsilon \rightarrow 0$, this corresponding to an ‘honest’ N -body calculation. However, the effects of a nonzero ϵ were also considered in some detail, with the aim of ascertaining possible undesirable consequences for conventional N -body simulations, which typically involve a substantial softening. The experiments with variable ϵ indicated that, for $\epsilon < 10^{-4}$ or so, the precise value of ϵ was largely immaterial, at least statistically.

III. SHORT TIME LYAPUNOV EXPONENTS

The principal diagnostic here was the mean (short time) Lyapunov exponent $\langle \chi \rangle$, generated, for a given choice of initial condition and for specified values of ϵ and N , as the average value of χ at $t = 100t_D$ for 20 different frozen- N potentials. The fundamental question was how, for fixed initial condition, this $\langle \chi \rangle$ depends on ϵ and N .

FIGURE 1 exhibits $\langle \chi \rangle$ as a function of $\log_{10} \epsilon$ for multiple integrations of one representative initial condition, which corresponded initially to a roughly isotropic distribution of velocities, allowing for several different values of N . FIGURE 2 gives $\langle \chi \rangle$ as a function of $\log_{10} N$ for the same initial condition, now allowing for several different values of ϵ .

It is evident from FIGURE 1 that, at least for comparatively large values of softening parameter, decreasing ϵ tends to make the orbit more chaotic. This is hardly surprising: Since the smooth potential is integrable, one anticipates that the chaos is associated completely with close encounters between the test mass and individual frozen masses. The introduction of a nonzero smoothing corresponds *de facto* to the introduction of a minimum impact parameter (since the potential is bounded in magnitude by $V_{max} = -GM/N\epsilon$) but the existence of such a minimum impact parameter limits the maximum effect that can arise from a close encounter.

However, for sufficiently small values of ϵ , the precise value of ϵ appears to be largely immaterial. This again is hardly surprising: As long as ϵ is small compared with the value of the closest separation between the test particle and any of the frozen particles during the course of the integration, the test particle feels an essentially unsoftened potential and should behave (at least statistically) as if $\epsilon = 0$. The point then is that, for $N \leq 10^6$ and an integration time as short as $100t_D$, the minimum separation associated with the closest encounter between the test mass and any of the frozen masses should be greater than or comparable to $\epsilon \sim 10^{-4}$. Indeed, a simple geometric argument indicates [9] that the time scale t_ϵ for a close encounter with minimum separation as small as ϵ scales as

$$\frac{t_\epsilon}{t_D} \sim \frac{R_{sys}^2}{N\epsilon^2}, \quad (3.1)$$

where R_{sys} is the size of the system in question.

One obvious implication of these results is that the introduction of a large amount of softening into a numerical simulation can have the unnatural result of significantly decreasing the amount of chaos manifested by individual orbits in a real astronomical system.

For comparatively large values of ϵ , $\langle \chi \rangle$ decreases rapidly with increasing N but, for sufficiently small values of N , it appears that $\langle \chi \rangle$ is nearly independent of N (although there are hints that $\langle \chi \rangle$ may continue to *increase* very slowly). The fact that, for large ϵ , $\langle \chi \rangle$ should decrease with increasing N can again be explained by comparing the magnitude of ϵ with the typical distance between masses in the system, which is of order $n^{-1/3} \sim R_{sys}/N^{1/3}$, with n a characteristic number density. If ϵ is larger than, or comparable to, $n^{-1/3}$, even weak close encounters are essentially ‘turned off,’ so that the source of chaos has been largely reduced, if not completely removed. The fact that $\langle \chi \rangle$ should be essentially independent of N in the limit $\epsilon \rightarrow 0$ has been argued

by various authors in a number of different ways [2,3]. A simple physical explanation is provided in the concluding section.

If a single orbit be integrated for progressively longer times, how quickly will the short time Lyapunov exponent $\chi(t)$ converge towards the true time-independent χ ? Studies of orbits in smooth nonintegrable potentials reveal that, when the phase space is highly complex and, because of the Arnold web, orbits can be ‘stuck’ temporarily in regions where the short time Lyapunov exponents are especially small or especially large, the time required for a reasonable level of convergence can be extremely long, $\sim 10^5 t_D - 10^6 t_D$ or even more [8]. If, however, the phase space is simpler in the sense that the Arnold web forms less of an impediment and such trapping is comparatively rare, the time required is typically much shorter. One way in which to quantify the overall rate of convergence is by performing a simple time series analysis: An orbit segment of length T can of course be divided into k segments of length $\Delta t = T/k$ and a short time Lyapunov exponent $\chi(\Delta t)$ computed for each segment. The dispersion $\sigma_\chi(\Delta t)$ then provides a useful probe of the degree to which, on time scales $\sim \Delta t$, the degree of chaos exhibited by different orbit segments is more or less the same. Determining σ_χ as a function of Δt provides a quantitative characterisation of the rate of convergence towards a unique χ_∞ . A simple argument based on the Central Limits Theorem suggests [10] that, if the accessible phase space regions are simple and trapping is rare, so that the amounts of chaos manifested at times t and $t + \Delta t$ are essentially uncorrelated,

$$\sigma_\chi \propto (\Delta t)^{-p}, \quad (3.2)$$

with $p = 1/2$. If, alternatively, the phase space is complex and trapping is important, one would expect that σ_χ decreases much more slowly with increasing Δt .

Such a time series analysis was performed for the data sets used to generate the mean exponents $\langle \chi \rangle$. For each set of 20 integrations, each orbit segment of length $T = 100t_D$ was separated into k segments of length $\Delta t = T/k$. A short time Lyapunov exponent $\chi(\Delta t)$ was then computed for each of the resulting $20k$ segments, and these were used to compute the dispersion $\sigma_\chi(\Delta t)$. Allowing for $k = 2^q$, for $q = 0, 1, 2, 3, 4, 5$, and 6 was equivalent to varying Δt between $\Delta t = (100/64)t_D$ and $\Delta t = 100t_D$. This time series analysis led to the conclusion that the dispersion σ_χ is typically well fit by a power law dependence of the form given by eq. (3.2), although the exponent p tends to be somewhat smaller than $p = 1/2$, the best fit value typically satisfying $p \sim 0.4$. Several examples are exhibited in FIGURE 3. The fact that p is comparatively close to $1/2$, rather than the much smaller values that are often observed in very ‘sticky’ nonintegrable potentials [10], corroborates the intuition that, because the chaos in this problem is associated exclusively with close encounters, trapping is rare and the degree of chaos exhibited at different times tends to be statistically uncorrelated.

IV. COMPARISON OF SMOOTH AND N-BODY ORBITS

It is clear that, for sufficiently short times, a frozen- N orbit will coincide almost exactly with the smooth potential characteristic associated with the same initial condition. And similarly, it is clear that, at sufficiently late times, the irregularities in the frozen- N potential will cause the frozen- N orbit to deviate significantly from the smooth characteristic. Probing the validity of the continuum limit at the level of individual orbits thus devolves into determining the rate at which the frozen- N orbits and smooth characteristics diverge. In this connection, two obvious questions arise. Do frozen- N orbits diverge from the smooth characteristics exponentially or as a power law in time? And how does the overall rate of divergence depend on N ?

Such probes of the validity of the continuum limit differ from the ordinary point of view, where convergence is typically defined in terms of quantities like bulk moments of the system, ignoring completely the behaviour of individual trajectories. A possible intermediate characterisation is to focus *not* on the pointwise behaviour of the chaotic orbits but, instead, on quantities which might be less sensitive to the N -body chaos. In particular, one can also ask: How do frozen- N orbits deviate from smooth characteristics in terms of quantities which, in the smooth potential, correspond to time-independent constants of the motion, like angular momentum in a spherically symmetric system?

These questions were addressed here both visually and quantitatively through a computation of the statistical properties of frozen- N orbits. Given $n = 20$ different trajectories $\{(\mathbf{r}_i(t), \mathbf{v}_i(t))\}$, $i = 1, \dots, n$, and the smooth characteristic $(\mathbf{r}_s(t), \mathbf{v}_s(t))$ associated with the same initial condition, there are two types of moments which one might choose to consider. Quantities like

$$\langle \mathbf{r} \rangle = \frac{1}{n} \sum_{i=1}^n \mathbf{r}_i \quad (4.1)$$

and

$$Dr^2 = \langle |\mathbf{r}_i - \langle \mathbf{r} \rangle|^2 \rangle \equiv \frac{1}{n} \sum_i |\mathbf{r}_i - \langle \mathbf{r} \rangle|^2 \quad (4.2)$$

and the corresponding quantities generated from \mathbf{v} and $\mathbf{J} = \mathbf{r} \times \mathbf{v}$ focus on the frozen- N orbits in and of themselves. Alternatively, such moments as

$$\Delta r^2 \equiv \langle |\mathbf{r} - \mathbf{r}_s|^2 \rangle = \frac{1}{n} \sum_i |\mathbf{r}_i - \mathbf{r}_s|^2 \quad (4.3)$$

and

$$\delta r^2 = \langle |\langle \mathbf{r} \rangle - \mathbf{r}_s|^2 \rangle \quad (4.4)$$

compare the frozen- N orbits with the smooth potential characteristic and, as such, their behaviour as a function

of N is particularly relevant in understanding the continuum limit. Overall, the quantities Dr , δr , and Δr were found to exhibit comparatively similar evolutions, so that attention below focuses on the moments $\langle \mathbf{r} \rangle$ and Δr , which seem especially natural physically.

The most striking conclusion is that individual frozen- N orbits typically diverge from the smooth characteristic as a power law in time, *not* exponentially. This is true both for comparatively large values of ϵ , where the frozen- N orbits are nearly regular, and for smaller values of ϵ , where the orbits are much more chaotic. This result is perhaps surprising. One might naively have supposed that, since the frozen- N orbits are strongly chaotic, at least for small ϵ , they would tend to diverge exponentially from the smooth characteristics on a time scale $\tau \sim \chi^{-1}$. However, such an exponential divergence is most definitely *not* observed.

For how long does this power law divergence persist? Does it cease when the distance between the frozen- N orbit and the smooth characteristic is still small, or does the divergence continue until the frozen- N orbit and the smooth characteristic tend to be widely separated in configuration space? If, *e.g.*, this divergence terminated at comparatively small separations, much smaller than the size of the system, one could argue that, even though the frozen- N orbits are chaotic, they still remain ‘close’ to the smooth characteristics. The answer here is that this divergence continues until the typical separation has become comparable to the size of the configuration space region to which the orbits are confined and the frozen- N orbit has become completely ‘decorrelated’ in appearance from the smooth potential characteristic.

The same conclusion also obtains if one focuses on an ensemble of 20 frozen- N orbits and probes their statistical properties. The six panels of FIGURE 4, generated for the initial condition used in FIGURES 1 - 3, compare $\langle x \rangle$ for frozen- N ensembles with the smooth x_s for orbits evolved with $\epsilon = 10^{-5}$, allowing for six values of N extending from $N = 316$ to $N = 100000$. In each case, one finds that, for sufficiently large t , $\langle x \rangle \rightarrow 0$, as would be expected if the frozen- N orbits have become completely different from one another and move through configuration space with random orientations. FIGURE 5 compares the radial coordinates $\langle r \rangle$ and r_s for the extreme case of an initial condition corresponding in the smooth potential to a purely radial orbit.

The time scale t_G on which the frozen- N orbits diverge from the smooth characteristic, and hence the time scale on which Δr grows, increases with increasing N . Even though the frozen- N orbits remain ‘equally chaotic’ in the sense that their Lyapunov exponents χ remain nearly constant, they remain close to the smooth characteristic for progressively longer times.

The left hand panels of FIGURE 6 exhibit $\Delta r/2^{1/2}R_s$, with R_s^2 the mean value of r^2 associated with the smooth characteristic, as computed for the same initial condition evolved with $\epsilon = 10^{-4}$ for $N = 1000$ and $N = 100000$. The right hand side exhibits the same data, recorded

at intervals of $0.025t_D$, once they have been subjected to a boxcar averaging over an interval $\delta t = 1t_D$. The large envelopes associated with the curves in the left hand panels reflect, *e.g.*, the fact that, at late times, individual orbits in the $n = 20$ orbit ensembles are oscillating about a value of unity.

That $\Delta r/2^{1/2}R_s$ converges towards unity is a reflection of the fact that the orbits have indeed become completely different one from another: Given that the frozen- N orbits conserve energy, one might expect that their average distance from the origin should, on the average, be the same as for the smooth characteristic, so that

$$\langle r^2(t) \rangle \rightarrow R_s^2 \quad \text{for} \quad t \rightarrow \infty. \quad (4.5)$$

Assuming, however, that this be true and that

$$\langle \mathbf{r}(t) \cdot \mathbf{r}_s(t) \rangle \rightarrow 0 \quad \text{for} \quad t \rightarrow \infty, \quad (4.6)$$

one infers that $\Delta \mathbf{r}^2 \rightarrow 2R_s^2$. Analogous behaviour is observed for the quantity $\Delta v/2^{1/2}V_s$, with V_s^2 defined correspondingly for the smooth characteristic.

As is manifested by FIGURE 6, the growth of Δr and Δv is roughly linear in time. Indeed, when comparing an ensemble of frozen- N orbits with a smooth orbit characteristic generated from the same initial condition, one finds that, for small ϵ , Δr and Δv are both reasonably well fit by a linear growth law of the form

$$\frac{\Delta r}{r_s} = \frac{\Delta v}{v_s} = \frac{t}{t_G}. \quad (4.7)$$

The growth time t_G , which is the same for both Δr and Δv , satisfies

$$t_G \approx A_G N^p t_D, \quad (4.8)$$

with A_G of order unity and $p \approx 1/2$. FIGURE 7 exhibits $\log_{10}(t_G/t_D)$ as a function of $\log_{10} N$ for two different initial conditions evolved with $\epsilon = 10^{-5}$.

The fact that t_G scales as $N^{1/2}$ would suggest that the divergence of the frozen- N orbits from smooth characteristics reflects a diffusion process, associated with a collection of random close encounters. However, this might in turn suggest that Δr and Δv should grow as $t^{1/2}$, rather than the approximately linear growth that was observed in the numerical simulations. Interesting, though, such a $t^{1/2}$ behaviour *does* obtain for quantities like angular momentum, which are conserved absolutely in the smooth potential. Indeed, one finds that, for small ϵ , ΔJ satisfies

$$\frac{\Delta J^2}{J_s^2} = \frac{t}{t_J}, \quad (4.9)$$

where J_s is the typical magnitude of the angular momentum associated with a characteristic with the specified energy. The growth time t_J again scales as $N^{1/2}$, but tends to be somewhat larger than t_G , so that

$$t_J \approx A_J N^p t_D, \quad (4.10)$$

with $A_J \sim 3A_G$ and $p \approx 1/2$. FIGURE 8 exhibits $\log_{10}(t_J/t_D)$ as a function of $\log_{10} N$ for the same integrations used to generate FIGURE 7.

There is also a clear visual sense in which, as N increases, the frozen- N orbits become progressively more regular in appearance. This is, *e.g.*, evident in FIGURE 9, which exhibits the x - y projections of representative frozen- N orbits with N varying between $N = 316$ and $N = 316228$, all generated from the same initial condition and integrated for a time $t = 25t_D$ with $\epsilon = 10^{-5}$. The final panel exhibits the smooth characteristic associated with the same initial condition. The most obvious point is that, as N increases, the configuration space region to which the orbit is restricted more closely coincides with the region occupied by the characteristic. For example, only for the three largest values of N is the orbit ‘centrophobic’ in the same sense as the characteristic.

Also evident is the fact that the orbit ‘looks smoother’ for larger values of N . This visual impression reflects the fact that, as N increases, the power associated with the Fourier spectrum of an orbit tends to become more concentrated near a few special frequencies. (Since the smooth orbit associated with the same initial condition is regular, all its power is concentrated at a countable set of discrete frequencies.) This trend is illustrated in the eight panels of FIGURE 10, each of which exhibits $|x(\omega)|$ for a single frozen- N orbit generated from the same initial condition. In each case, the data are so normalised that the peak frequency has $|x(\omega)| = 1$. The spectra were generated from a time series of 4001 points, recorded at intervals of $0.025t_D$.

The degree to which the orbits become more nearly regular with increasing N can be quantified by determining [11] the ‘complexity’ of the orbits, *i.e.*, the number of frequencies in the discrete Fourier spectrum which contain an appreciable amount of power. Two such measures of complexity are illustrated in FIGURE 11, which was computed for ensembles of frozen- N orbits with varying N , all evolved with $\epsilon = 10^{-5}$ and generated from the same initial condition. The solid curve exhibits $f_{0.1}$, defined as the sum of the numbers of frequencies $f_{0.1,x}$, $f_{0.1,y}$, and $f_{0.1,z}$ which have more than 10% as much power as the peak frequencies for ω_x , ω_y , and ω_z , *i.e.*,

$$f_{0.1} = f_{0.1,x} + f_{0.1,y} + f_{0.1,z}. \quad (4.11)$$

The dashed curve exhibits $k_{0.95}$, defined correspondingly as the sum of the numbers of frequencies required to capture 95% of the power in the x -, y -, and z -directions. In each case, the curve represents an average over different orbits in the ensemble, and the error bars represent the associated dispersions. The obvious point is that both these quantities decrease with increasing N .

The fact that, as N increases, power becomes more concentrated near a few special frequencies has important implications for various physical processes which rely on resonances. For example, a variety of recent arguments in both galactic and solar system dynamics invoke a process of so-called ‘resonant relaxation,’ [12] which relies

on the assumption that, in the presence of a large central object (a supermassive black hole in the center of a galaxy or the Sun at the center of the solar system), N -body orbits behave very nearly as if they were Keplerian trajectories in the fixed $1/r$ potential associated with the central object. If the chaos exhibited by individual orbits [13] implied that these orbits were highly irregular, so that their power was not concentrated near the special Keplerian frequencies, resonant relaxation might seem quite implausible. Given, however, that the orbits become progressively more regular for increasing N , resonant relaxation would seem eminently reasonable, at least for systems in which N is sufficiently large.

V. CONCLUSIONS AND DISCUSSION

Even though trajectories remain chaotic in the sense that the largest Lyapunov exponent does not decrease towards zero, there is a clear sense in which, for increasing N , orbits in frozen- N potentials exhibit a pointwise convergence towards characteristics in the smooth potential which the frozen- N potentials were chosen to sample. Viewed in configuration or velocity space, frozen- N orbits tend to diverge linearly from the smooth characteristic with the same initial condition on a time scale t_G that is proportional to $N^{1/2}$. In this sense, the continuum limit appears justified even at the level of individual trajectories. The fact that frozen- N orbits remain chaotic for very large N is completely consistent with the existence of a well-defined continuum limit.

It is easy to understand qualitatively why the frozen- N orbits should remain chaotic even for very large N . Given that the chaos disappears completely in the continuum limit, where the orbits reduce to integrable characteristics, it would seem clear that the chaos must be associated with a sequence of ‘random’ interactions between a ‘test’ particle and a collection of ‘field’ particles. However, this would suggest that the time scale associated with the growth of a small initial perturbation can be estimated by considering the tidal effects associated with a pair of particles separated by a distance comparable to the typical interparticle separation. This tidal acceleration will of course scale as

$$\delta\ddot{\mathbf{r}} = (\delta\mathbf{r} \cdot \nabla) \mathbf{a} \sim \frac{Gm}{r^3} \delta\mathbf{r}, \quad (5.1)$$

with r the separation and m the particle mass. Given, however, that $r \sim n^{-1/3} \sim N^{-1/3} R_{sys}$, with n a characteristic number density and R_{sys} the size of the system, it follows that the time scale t_* associated with the interaction should satisfy

$$t_* \sim 1/\sqrt{G\rho}. \quad (5.2)$$

In other words, the time scale associated with any orbital instability induced by the graininess of the system should be comparable to the dynamical time t_D , independent

of particle number N . As N increases, the size of the individual particle mass, m , and the cube of the typical separation between particles, $\sim n^{-1}$, both decrease as N^{-1} so that their ratio is independent of particle number.

The fact that the chaotic frozen- N orbits appear to become “more nearly regular” as N increases is consistent with recent claims that the “scale” associated with N -body chaos decreases with increasing N . Specifically, by comparing trajectories associated with two nearby initial conditions evolved in the same frozen- N potential, Val-
luri and Merritt [14] found that, when scaled in terms of R_{sys} , the size of the system, the typical separation R_{sat} on which the initial exponential divergence saturates decreases with increasing particle number, so that R_{sat}/R_{sys} is a decreasing function of N .

That the rate of divergence in the nonlinear regime slows more and more for larger N can be quantified by tracking the actual evolution of two orbits generated from nearby initial conditions and determining the time required before their separation becomes ‘macroscopic.’ The result of such an investigation is illustrated in FIGURE 12, which was generated once again from ensembles of 20 frozen- N orbits all evolved with $\epsilon = 10^{-5}$. In each case, the unperturbed orbits were identical to those used to generate FIGURE 1; the perturbed orbits involved changing the initial value of x by an amount $\delta x = 10^{-6}$. FIGURE 12 exhibits as a function of N the mean time τ required before the separation

$$\delta r = (\delta x^2 + \delta y^2 + \delta z^2)^{1/2} \quad (5.3)$$

had achieved the value $\delta r = 1$. (For this initial condition, the average value of r associated with the smooth characteristic was $R_s \approx 1.83$.) The error bars were derived by considering the first and second ten orbits in the ensemble separately. Because individual orbits diverge at vastly different rates, the dispersion associated with a 20 orbit ensemble is much larger than reflected by these error bars. It is clear that τ increases systematically with increasing N , although considerably more slowly than with the $N^{1/2}$ dependence observed for the divergence time scales t_G and t_J .

When viewed in terms of collisionless invariants like angular momentum, the divergence of frozen- N orbits from smooth characteristics with the same initial condition is well approximated as a diffusion process, in which ΔJ grows as $(t/t_J)^{1/2}$ and where, for fixed t_D , the divergence time scale t_J varies at least approximately as $N^{1/2}$. This reinforces the conventional wisdom [15] that discreteness effects may be modeled as white, or nearly white, Gaussian noise in the context of a Langevin or Fokker-Planck description. It might, therefore, seem somewhat surprising that, although the divergence time scale t_G in configuration or velocity space again scales as $N^{1/2}$, the quantities Δr and Δv grow *linearly* in time, rather than as $t^{1/2}$.

In this regard, it is significant that if the smooth Plummer potential be replaced by the smooth potential associated with a constant density configuration, the linear

growth exhibited Δr and Δv is in fact replaced by the ‘expected’ diffusive behaviour. In this case Δr and Δv both grow as $t^{1/2}$, and, when expressed in units of the dynamical time t_D , the growth time t_G is somewhat longer, corresponding more nearly to the time scale t_J associated with ΔJ .

This suggests strongly that the behaviour of Δr and Δv observed for the Plummer potential is associated with linear phase mixing. Because of finite number statistics, the same initial condition $(\mathbf{r}_0, \mathbf{v}_0)$ in different frozen- N realisations of a Plummer potential will correspond to somewhat different energies, the values of which are conserved in the subsequent evolution. However, even neglecting discreteness effects, initially proximate orbits in a generic integrable potential will, if their energies be unequal, tend to diverge linearly. For example, two orbits evolved in a smooth Plummer potential with the same initial \mathbf{r} but slightly different values of \mathbf{v} and, hence, slightly different energies, will oscillate with somewhat different frequencies and, as a result, exhibit an overall linear divergence. If, however, the orbits are evolved instead in the potential associated with a constant density distribution, this is no longer true. A constant density sphere corresponds to a harmonic potential, where all orbits have the same unperturbed frequencies; and, for this reason, orbits in the smooth potential with slightly different energies will not exhibit such a systematic divergence.

The fact that frozen- N orbits look “more nearly regular” for large N suggests that the chaos associated with discreteness effects in the N -body problem should be viewed very differently from the chaos associated with a bulk nonintegrable potential. When evolved into the future, two nearby chaotic initial conditions in such a potential tend to diverge exponentially until they are separated by a distance comparable to the size of the easily accessible (*i.e.*, not significantly impeded by the Arnold web) connected phase space region to which the orbits are confined, a region which tends, typically, to be macroscopic. By contrast, the scale associated with chaos induced by discreteness effects in the N -body problem is distinctly microscopic, at least for comparatively large N . It would appear that any single orbit with fixed energy can access a phase space region which is in fact very large; but the chaos which it experiences is a superposition of short range effects with characteristic scale $\ll R_{sys}$.

ACKNOWLEDGMENTS

The authors acknowledge useful discussions with Alexei Fridman, Salman Habib, and Ilya Pogorelov. This research was supported in part by NSF AST-0070809 and by the Institute for Geophysics and Planetary Physics at Los Alamos National Laboratory.

[1] R. H. Miller, *Astrophys. J.* **140**, 250 (1964).

[2] H. E. Kandrup, *Physica A* **169**, 73 (1989).

[3] J. Goodman, D. Heggie, and P. Hut, *Astrophys. J.* **415**, 715 (1993).

[4] Cf. H. E. Kandrup, M. E. Mahon, and H. Smith, *Astrophys. J.* **428**, 458 (1994), and references cited therein.

[5] Cf. J. Binney and S. Tremaine, *Galactic Dynamics* (Princeton University Press, Princeton, 1987).

[6] Cf. H. E. Kandrup and H. Smith, *Astrophys. J.* **374**, 255 (1991).

[7] S. J. Aarseth, M. Hénon, and R. Wielen, *Astron. Astrophys.* **37**, 183 (1974).

[8] Cf. A. J. Lichtenberg and M. A. Lieberman, *Regular and Chaotic Dynamics* (Springer, Berlin, 1992).

[9] Cf. eq. (7.7) in H. E. Kandrup, *Phys. Reports.* **63**, 1 (1980).

[10] C. Siopis and H. E. Kandrup, *Mon. Not. Roy. Astro. Soc.* **319**, 43 (2000).

[11] Cf. H. E. Kandrup, B. L. Eckstein, and B. O. Bradley, *Astron. Astrophys.* **320**, 65 (1997), which discusses the pros and cons of the admittedly somewhat simplistic probes of ‘complexity’ used in this paper.

[12] K. P. Rauch and S. Tremaine, *New. Astron.* **1**, 149 (1996).

[13] A numerical investigation of the N -body problem in the presence of a much larger central point mass (H. Smith, H. E. Kandrup, M. E. Mahon, and C. Siopis, in *Ergodic Concepts in Stellar Dynamics*, edited by V. G. Gurzadyan and D. Pfenniger, Springer Lectures Notes in Physics No. 430 (Springer, New York, 1994), p. 158) suggests that, even if the central mass M_{BH} is much larger than the total mass $M = Nm$ of the individual particles, the N -particle orbits continue to exhibit a sensitive dependence on initial conditions. For example, for orbits in simulations with $M_{BH} = 10M$, the characteristic time scale t_* associated with the exponential sensitivity was found to be less than three times longer than the value of t_* for $M_{BH} = 0$.

[14] M. Valluri and D. Merritt, in *The Chaotic Universe*, edited by R. Ruffini and V. G. Gurzadyan (World Scientific, New York, 1999).

[15] Cf. S. Chandrasekhar, *Rev. Mod. Phys.* **15**, 1 (1943).

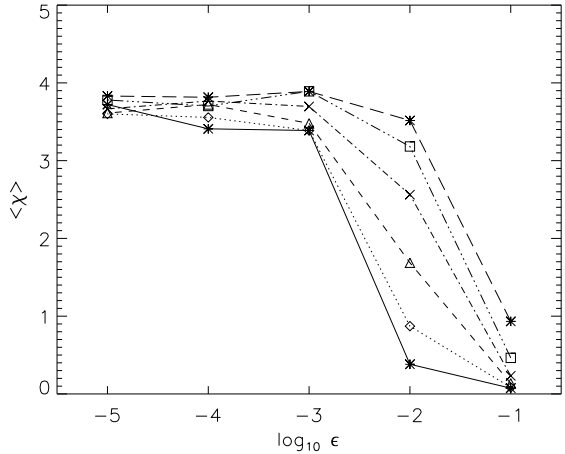


FIG. 1. Mean short time Lyapunov exponent $\langle \chi \rangle$ as a function of softening parameter ϵ for $N = 10^5$ (solid line), $N = 10^{4.5}$ (dotted), $N = 10^4$ (dashed), $N = 10^{3.5}$ (dot-dashed), $N = 10^{3.0}$ (triple-dot dashed), and $N = 10^{2.5}$ (broad dashed). The integrations were all performed for a single ‘typical’ initial condition.

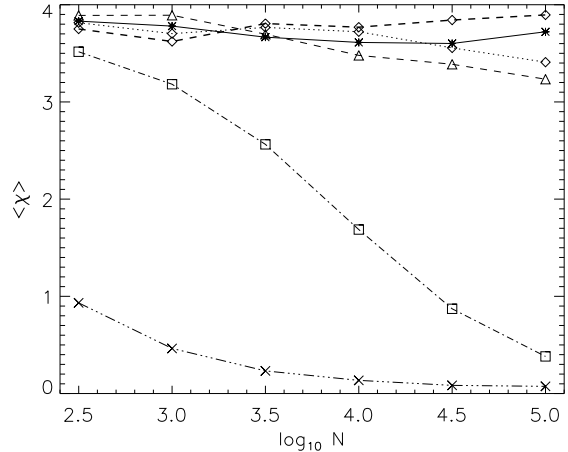


FIG. 2. Mean short time Lyapunov exponent $\langle \chi \rangle$ as a function of particle number N for $\epsilon = 10^{-5}$ (solid line), $\epsilon = 10^{-4}$ (dotted), $\epsilon = 10^{-3}$ (thin-dashed), $\epsilon = 10^{-2}$ (dot-dashed), and $\epsilon = 10^{-1}$ (triple-dot dashed), all computed for the initial condition used to generate FIG. 1. The short time $\langle \chi \rangle$ for a different initial condition corresponding to a smooth radial orbit, again evolved with $\epsilon = 10^{-5}$, is indicated by the curve with thick dashes.

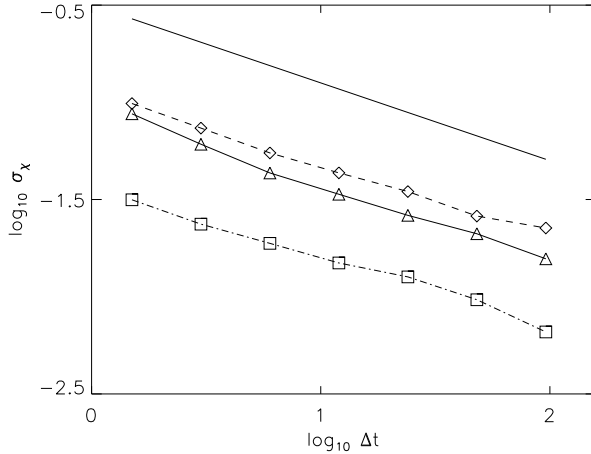


FIG. 3. $\log_{10} \sigma_x(\Delta t)$ as a function of $\log_{10} \Delta t$ for three sets of simulations: $N = 31623$ and $\epsilon = 0.0001$ (solid curve), $N = 316$ and $\epsilon = 0.0001$ (dashed curve), and $N = 316$ and $\epsilon = 0.1$ (dot-dashed curve), all computed for the initial condition used to generate FIG. 1. The thick solid line has a slope corresponding to $p = 0.4$.

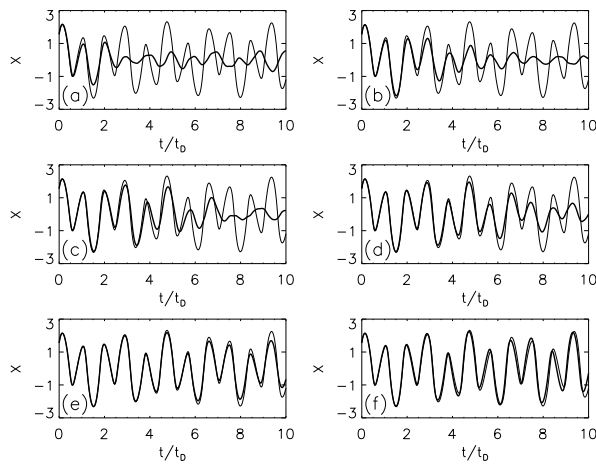


FIG. 4. (a) The trajectory $x_{sm}(t)$ in the smooth potential (thin curve) and the mean trajectory $\langle x(t) \rangle$ (thick curve) derived from 20 frozen- N simulations with $N = 316$ and $\epsilon = 10^{-4}$, performed for the initial condition used to generate FIG 1. (b) The same for $N = 1000$. (c) $N = 3162$. (d) $N = 10000$. (e) $N = 31623$. (f) $N = 100000$.

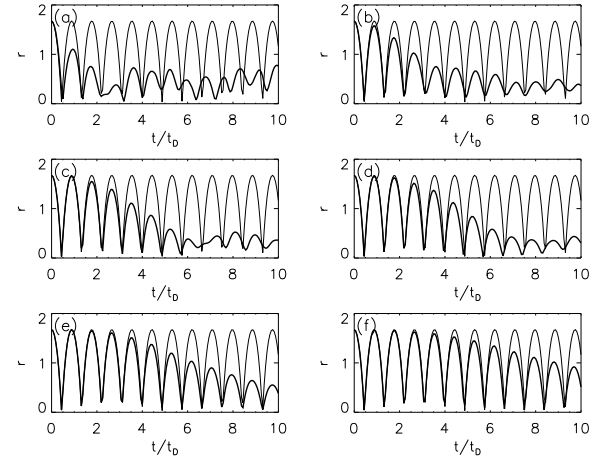


FIG. 5. (a) The radial coordinate $r_s(t)$ in the smooth potential (thin curve) and the mean trajectory $\langle r(t) \rangle$ (thick curve) derived from 20 frozen- N simulations with $N = 316$ and $\epsilon = 10^{-4}$, performed for an initial condition corresponding in the smooth potential to a purely radial orbit. (b) The same for $N = 1000$. (c) $N = 3162$. (d) $N = 10000$. (e) $N = 31623$. (f) $N = 100000$.

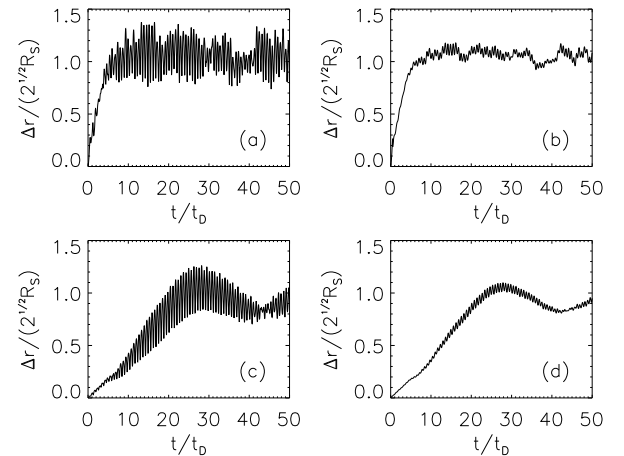


FIG. 6. (a) The quantity $\Delta r / \sqrt{2R_s^2}$ for frozen- N simulations with $N = 1000$ and $\epsilon = 10^{-4}$. (b) The same data subjected to boxcar averaging over an interval $t = t_D$. (c) and (d) The same for $N = 100000$.

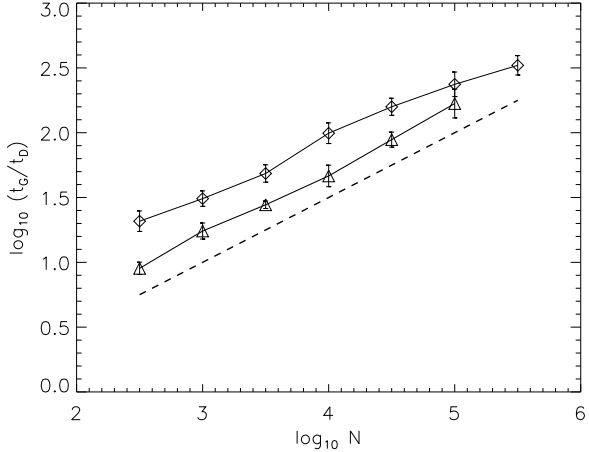


FIG. 7. Best fit values of the time scale $t_G(N)$ associated with the divergence of smooth and frozen- N orbits for two different initial conditions: $\Delta r/R_s = \Delta v/V_s \equiv t/t_G$. The dashed line has slope $1/2$, corresponding to an $N^{1/2}$ dependence.

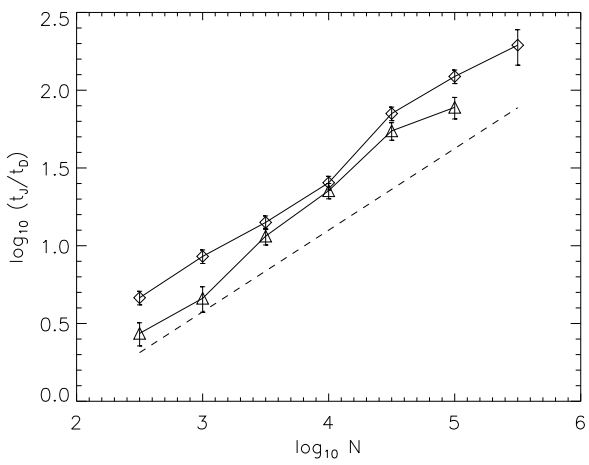


FIG. 8. Best fit values of the time scale $t_J(N)$ associated with changes in angular momentum for frozen- N orbits for two different initial conditions: $\Delta J^2/J_s^2 \equiv t/t_J$. The dashed line has slope $1/2$, corresponding to an $N^{1/2}$ dependence.

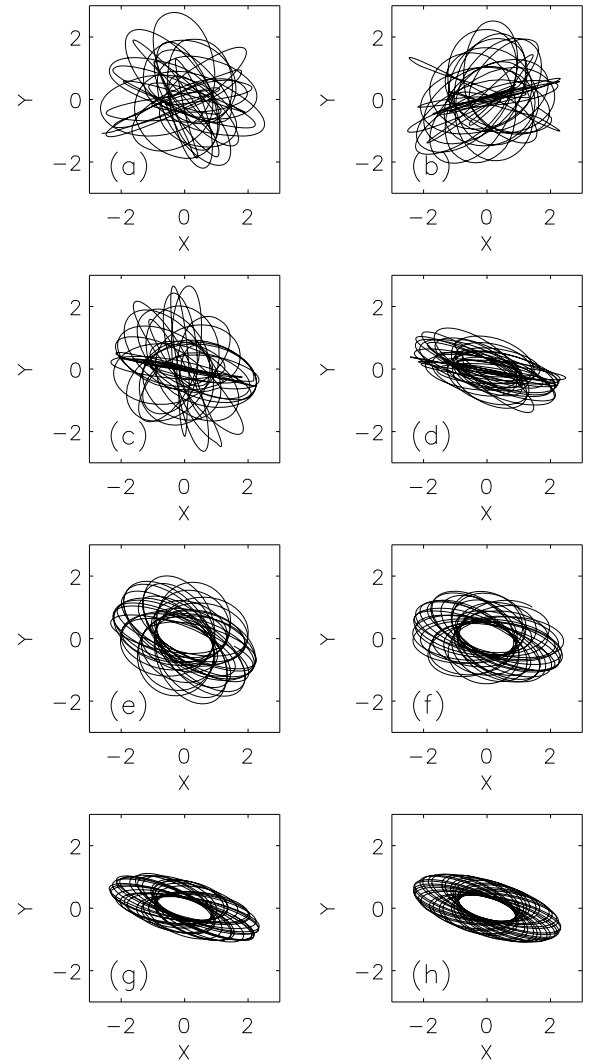


FIG. 9. The x - y projection of representative frozen- N orbits generated from the same initial condition, evolved for $t = 25t_D$ with $\epsilon = 10^{-5}$. (a) $N = 316$. (b) $N = 1000$. (c) $N = 3163$. (d) $N = 10000$. (e) $N = 31623$. (f) $N = 100000$. (g) $N = 316228$. (h) The x - y projection of the same initial condition evolved in the smooth potential

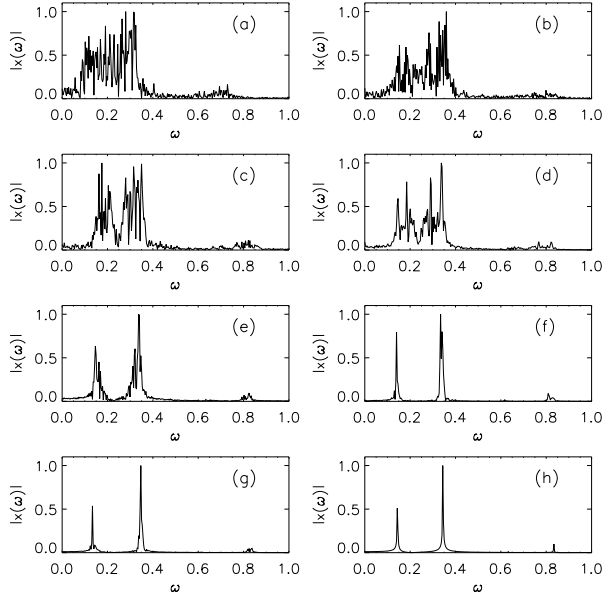


FIG. 10. (a) The Fourier transformed $|x(\omega)|$ for one frozen- N integration of the initial condition used to generate FIGURE 4, evolved with $\epsilon = 10^{-5}$ and $N = 316$. (b) The same for $N = 1000$. (c) $N = 3162$. (d) $N = 10000$. (e) $N = 31623$. (f) $N = 100000$. (g) $N = 316228$. (h) $|x(\omega)|$ for a characteristic in the smooth potential with the same initial condition, with data recorded at the same intervals for the same total integration time.

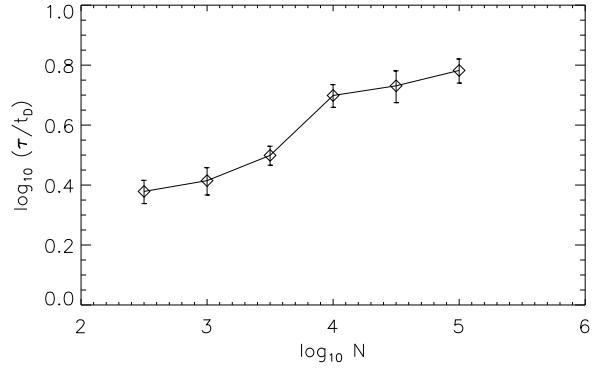


FIG. 12. The mean time required for two frozen- N orbits separated initially by a distance $\delta r = 10^{-6}$ to achieve a macroscopic separation $\delta r = 1$.

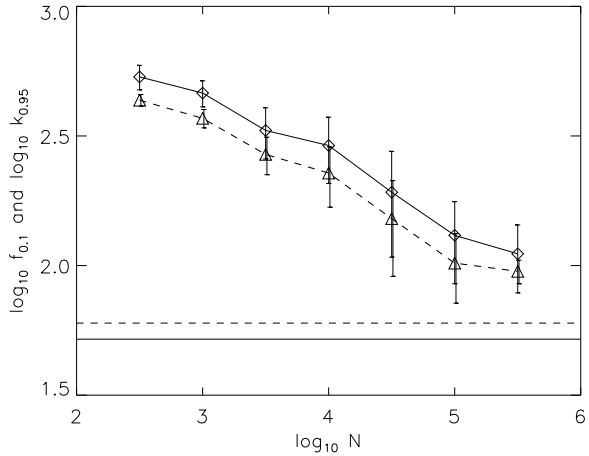


FIG. 11. Two probes of the complexity of frozen- N orbits for an ensemble of orbits with the same initial condition evolved with $\epsilon = 10^{-5}$. The solid curve exhibits $f_{0,1}$, the number of frequencies which have power equal to at least 10% of the power in the peak frequencies. The dashed curve exhibits $k_{0.95}$, the number of frequencies required to capture 95% of the total power. The vertical lines show $f_{0,1}$ and $k_{0.95}$ for a smooth characteristic generated identically from the same initial condition, thus exhibiting the intrinsic limitations associated with the discrete time series of data points.